Available online at www.sciencedirect.com
SCIENCE DIRECT®
Nuclear Instruments and Methods in Physics Research A 498 (2003) 352–361
NUCLEAR INSTRUMENTS & METHODS IN PHYSICS RESEARCH Section A
www.elsevier.com/locate/nima

Performances of a CeF_3 crystal scintillator and its application to the search for rare processes

P. Belli[a], R. Bernabei[a,*], R. Cerulli[a], C.J. Dai[b], F.A. Danevich[c], A. Incicchitti[d], V.V. Kobychev[c,e], O.A. Ponkratenko[c], D. Prosperi[d], V.I. Tretyak[c,d], Yu.G. Zdesenko[c]

[a] *Dipartimento di Fisica, Università di Roma "Tor Vergata" and INFN, Sezione di Roma II, I-00133 Rome, Italy*
[b] *IHEP, Chinese Academy, P.O. Box 918/3, Beijing 100039, People's Republic of China*
[c] *Institute for Nuclear Research, MSP 03680 Kiev, Ukraine*
[d] *Dipartimento di Fisica, Università di Roma "La Sapienza" and INFN, Sezione di Roma, I-00185 Rome, Italy*
[e] *INFN, Laboratori Nazionali del Gran Sasso – 67010 Assergi (AQ), Italy*

Received 16 August 2002; received in revised form 6 December 2002; accepted 10 December 2002

Abstract

The performances of a CeF_3 crystal scintillator with a mass of 49.3 g have been investigated. In particular, the α/β light ratio and the possibility of a pulse-shape discrimination between α particles and γ quanta have been studied. The radioactive contamination of the crystal has been investigated. The application of the obtained results in the search for rare processes such as the two neutrino double electron capture in ^{136}Ce and ^{138}Ce and the α activity in ^{142}Ce has been investigated. As a result, new $T_{1/2}$ limits for these processes have been determined (90% C.L.): $T_{1/2}^{2\nu2K}(^{136}\mathrm{Ce}) \geqslant 2.7 \times 10^{16}$ yr, $T_{1/2}^{2\nu2K}(^{138}\mathrm{Ce}) \geqslant 3.7 \times 10^{16}$ yr and $T_{1/2}^{\alpha}(^{142}\mathrm{Ce}) \geqslant 2.9 \times 10^{18}$ yr.

PACS: 23.40. − s; 23.60. + e; 29.40.Mc

Keywords: CeF_3 crystal scintillator; α/β ratio; Pulse shape discrimination; Double β decay; α decay; Ce isotopes

1. Introduction

During the last decade, CeF_3 crystals were regarded as one type of the most promising scintillators for the next generation experiments in high energy physics because of their high density, fast response and high radiation resistance. These scintillators are relatively new; in fact, their good characteristics were discovered for small (few cm^3) samples in 1989 [1]. During the following years, the properties of CeF_3 crystals were intensively investigated, in particular, by the Crystal Clear Collaboration (see Ref. [2] and references therein). The main characteristics are: (i) density equal to 6.16 g/cm^3; (ii) light yield

*Corresponding author. Dipartimento di Fisica, Università di Roma "Tor Vergata", Via della Ricerca Scientifica 1, Roma 00173, Italy. Tel./fax: +039-06-7259-4542.
E-mail address: bernabei@roma2.infn.it (R. Bernabei).

0168-9002/03/$ - see front matter
doi:10.1016/S0168-9002(02)02106-X

4–5% of that of NaI(Tl); (iii) refractive index equal to 1.62 at 400 nm; (iv) emission peaks at 286, 300 and 340 nm. Moreover, several decay components have been recognized: the most important ones have decay time equal to 5 and 30 ns, respectively. The material is non-hygroscopic; the melting point is at 1443°C; the light yield has only a small dependence on temperature (0.05%/°C); the thermal-neutron cross-section is equal to 0.65 barn, near 2 orders of magnitude lower than that of CsI [2].

CeF_3 crystals are interesting not only in high energy physics, but also in other fields of physics, such as in studies on double beta decay processes and on other rare nuclear decays. In particular, the first use of CeF_3 scintillators (containing two 2β candidate nuclei: ^{136}Ce and ^{138}Ce) for 2β decay studies was published in Ref. [3]; there two CeF_3 crystals (one 345 g produced by Preciosa–Crytur a Czech company and one 74.5 g produced by a Chinese company) were used.

While the optical properties of the CeF_3 crystals (light yield, scintillation mechanisms) and radiation resistence relevant for their use in high energy physics were thoroughly investigated [1,2], some other characteristics (important in low background experiments on the search for rare nuclear decays with typical energy release of a few MeV) have not yet been studied. Among them, there are the relative light yield for α particles compared to that for β particles or γ's (the so-called α/β ratio) and the possibility of a discrimination between α and β particles by exploiting the pulse-shape analysis. In the present paper, the spectroscopic properties and the pulse-shape discrimination capability of a new 49.3 g CeF_3 crystal scintillator recently produced in China[1] are investigated. The radioactive contamination of the CeF_3 crystal is also quantitatively studied—in our knowledge—for the first time. The results are then applied to the search for 2νEC/EC processes in ^{136}Ce and ^{138}Ce as well as for α activity in ^{142}Ce.

[1] Unfortunately, the detector's radiopurity in the present realization is poorer (see later) than that of the detectors available at time of the measurements of Ref. [3]. This further points out the relevant role of the manufacturing in the final radiopurity of the detector.

2. Detector and measurements

The measurements have been carried out in a low background set-up at the Gran Sasso National Laboratory of the I.N.F.N. The used CeF_3 crystal scintillator ($2 \times 2 \times 2$ cm^3, mass of 49.3 g) has been directly coupled to two low radioactive EMI9265FLB53 photomultipliers (PMT) with 3″ in diameter. The two PMTs work in coincidence.

The detector has been surrounded by Cu brick and sealed in a low radioactive Cu box continuously flushed with high purity nitrogen gas (stored deeply underground for a long time) to avoid presence of residual environmental radon. The Cu box has been surrounded by a passive shield made of 10 cm of high purity Cu, 15 cm of low radioactive lead, 1.5 mm of cadmium and 4 (10) cm polyethylene (paraffin) to reduce the external background. The whole shield has been closed inside a Plexiglas box, also continuously flushed by high purity nitrogen gas.

An event-by-event data acquisition system records the amplitude, the arrival time and the pulse shape (200 channels, 6.25 ns per channel) of each event.

The linearity of the detector energy scale and the behaviour of the energy resolution have been measured in the energy region 60−1275 keV with γ sources (^{22}Na, ^{57}Co, ^{137}Cs, ^{133}Ba and ^{241}Am). In particular, the measured energy dependence of the energy resolution can be expressed as $\mathrm{FWHM}_\gamma(\mathrm{keV}) = 5 + \sqrt{20E_\gamma}$, where E_γ is given in keV. The energy threshold of the spectrometer has been checked with the help of an ^{241}Am γ source (≈100% efficiency of registration at 60 keV and at least 95% at 45 keV).

3. α/β ratio of the CeF_3 detector

The relative light output for α particles as compared with that for β particles (or γ rays), named α/β ratio[2]—has been measured with a

[2] The detector energy scale is measured with γ sources, thus the notation "α/γ ratio" could be more adequate. However, because γ rays interact with matter by means of the energy transfer to electrons, in present paper we are using the traditional notation "α/β ratio".

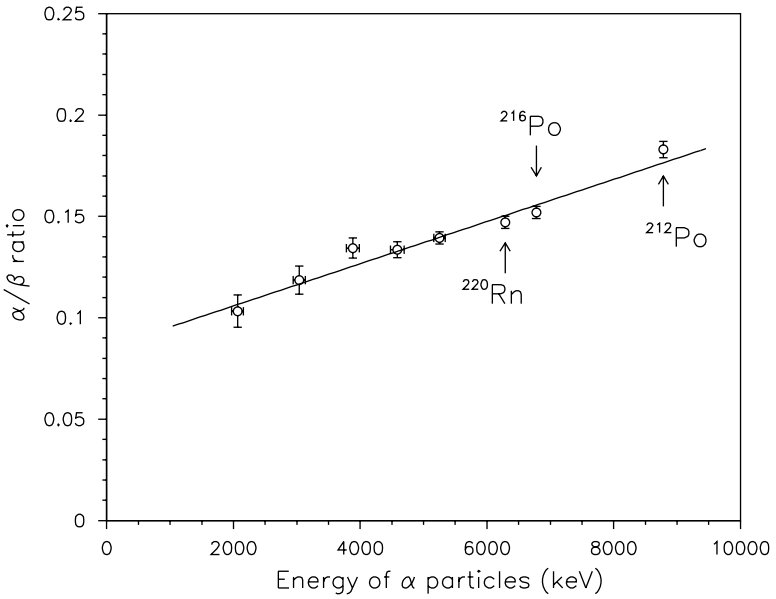

Fig. 1. Energy dependence of the α/β ratio for the CeF_3 scintillator as measured with an ^{241}Am alpha source. The points corresponding to the α peaks of ^{220}Rn and ^{216}Po have been selected by the time-amplitude analysis (see text and Fig. 5); the peak of ^{212}Po has been obtained by the pulse-shape analysis of the background data (see text and Fig. 3). Solid line represents the fitting curve of the experimental points.

collimated ^{241}Am α source. Such an α beam passed through thin absorbers of known thickness, thus the energy of the emerging α particles can precisely be calculated. Moreover, it has also been measured with the help of a surface-barrier Si semiconductor detector whose energy resolution was: FWHM = 0.6% at 5.25 MeV. The dimensions of the collimator are $\varnothing$ 0.75×2 mm and the thickness of a single mylar film absorber is 0.65 mg/cm^2. By using different sets of absorbers, α particles with energies 2.07, 3.04, 3.88, 4.58, and 5.25 MeV were obtained. Besides, alpha peaks of ^{220}Rn, ^{216}Po and ^{212}Po from the internal thorium contamination of the crystal[3] have also been used; this allows us to calibrate the detector in a wide energy range of α particles: from 2 to 8.8 MeV.

The derived energy dependence of the α/β ratio is shown in Fig. 1 and can be expressed as $\alpha/\beta = 0.084 + 1.09 \times 10^{-5} E_\alpha$, where E_α is in keV. The peaks obtained with the ^{241}Am source as well as the peaks of ^{220}Rn, ^{216}Po and ^{212}Po have also been used to determine the energy resolution of the detector for α particles ($FWHM_\alpha$); it is well described by the linear function: $FWHM_\alpha(\text{keV}) = 25 + 0.022 E_\alpha$.

Finally, the possible dependence of the crystal's light output on the direction of the α irradiation relatively to the crystal axis [4] has been investigated. To study this effect, the CeF_3 crystal has been irradiated by α particles in three directions perpendicular to the three crystal surfaces. No such a dependence of α/β ratio has been found in the CeF_3 crystal within the experimental errors.

4. Pulse-shape discrimination capability

Scintillation light pulses induced by α particles in the CeF_3 are modestly faster than those of γ quanta (β particles), allowing the discrimination between α and γ(β) events with the help of a pulse-shape discrimination technique. As it is well known, a similar feature is offered by various scintillators and we have already exploited it in

[3] The mentioned peaks were obtained from the experimental data with the help of the time-amplitude and pulse-shape analysis described below.

NaI(Tl) [5], in LXe [6] and in $CdWO_4$ [7]. Various analysis approaches can be considered; here, we have exploited in particular the optimal digital filter [8]. To obtain the numerical characteristic of the CeF_3 scintillation signal, namely the shape indicator (SI), the following formula was applied for each pulse: $SI = \sum f(t_k) \times P(t_k)$, where the sum is over k time channels starting from the origin of the signal up to 125 ns and $f(t_k)$ is the digitized amplitude of a given signal normalized to the area. The weight function $P(t)$ is defined as $P(t) = f_\alpha(t) - f_\gamma(t)$, where $f_\alpha(t)$ and $f_\gamma(t)$ are the reference light pulse shape for α particles and γ quanta, resulting from the average of a large number of individual events.

The pulse shapes of the CeF_3 crystal scintillator were investigated for γ rays in the energy range of 0.06−1.33 MeV (with ^{137}Cs and ^{60}Co sources) and for α particles in the energy range of 5.5−6.8 MeV (using α active impurities inside the crystal). The measured SI for γ quanta slightly depends on the energy: $SI_\gamma = 26.8 - 0.16 \times 10^{-3} E_\gamma$ (here and further SI and σ are dimensionless, and E_γ and E_α are expressed in keV). The scatter plot of the shape indicator versus energy for 20.9 h of background measurements with the used CeF_3 crystal is depicted in Fig. 2.

The population of the α events is slightly shifted relatively to that of the γ(β) events. As it is visible in the inset of Fig. 2, the distributions of the shape indicator for γ(β) and α events are well described by Gaussian functions. The energy dependence of the Gaussian standard deviation for γ quanta (σ_γ) has been obtained from the fit of the experimental data as $\sigma_\gamma = 0.7 + 122/\sqrt{E_\gamma}$. The $\pm 1\sigma_\gamma$ interval for SI_γ is also shown in Fig. 2. The corresponding parameters for the α particles with the 5.5−6.8 MeV energy are equal to $SI_\alpha = 30.2$ and $\sigma_\alpha = 4.8$.

Besides, due to the appreciable time difference between CeF_3 scintillation signal (≈30 ns) and PMT noise (≈5 ns), which results in a large SI

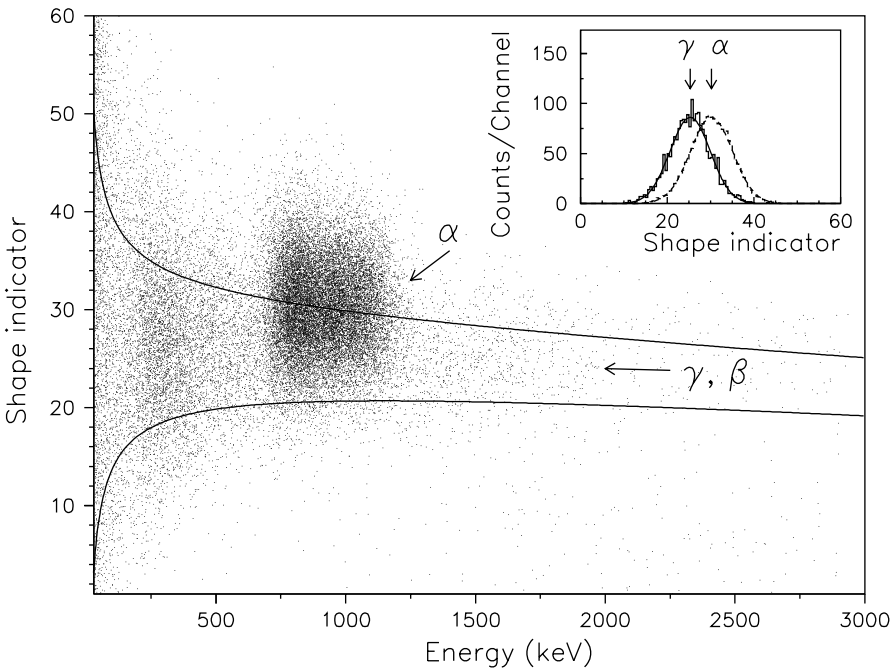

Fig. 2. Scatter plot of the shape indicator (see text) versus energy for 20.9 h of background exposition with the CeF_3 scintillation detector. One sigma interval for shape indicator values corresponding to γ quanta (β particles) is drawn. Points with lower SI values are due to events $^{212}Bi \rightarrow {}^{212}Po \rightarrow {}^{208}Pb$. In the inset: the distributions of the shape indicator measured for γ quanta and for α events selected from the background data.

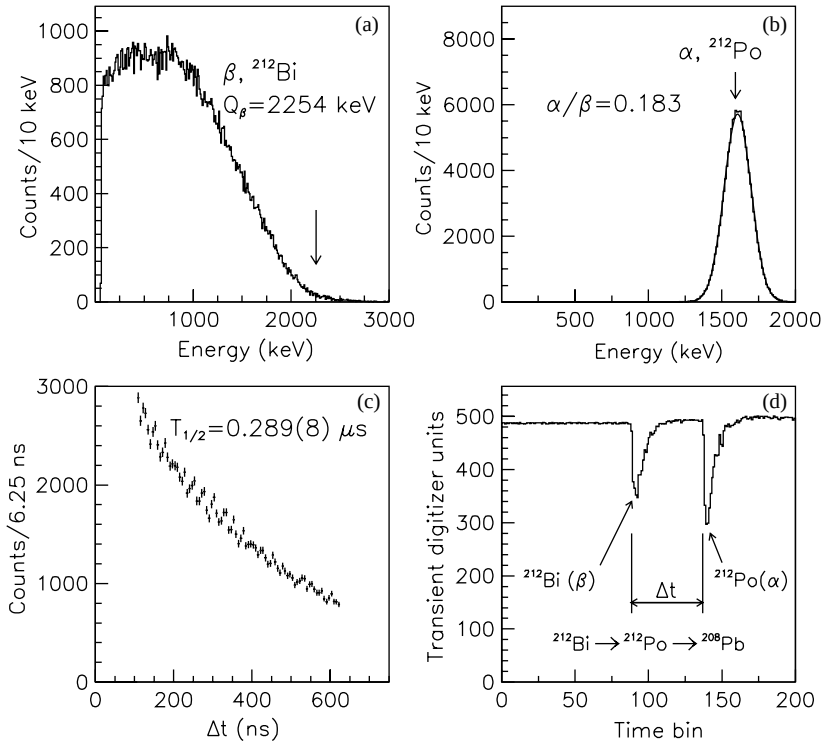

Fig. 3. The energy (a,b) and time (c) distributions of the fast sequence of β (^{212}Bi, $Q_\beta = 2254$ keV) and α (^{212}Po, $E_\alpha = 8784$ keV, $T_{1/2} = 0.299(2)$ μs [10]) decays selected by pulse-shape analysis from the background data recorded over 2142 h. The fit of the time distribution gives an half-life: $T_{1/2} = 0.289(8)$ μs, which is in good agreement with the result from literature for ^{212}Po [10]. (d) Example of such an event in the CeF_3 scintillator.

difference, the described filter is very useful to reject the PMT noise.

Another technique of background rejection has also been applied to the fast sequence of decays from the ^{232}Th family: ^{212}Bi ($Q_\beta = 2254$ keV)→ ^{212}Po ($E_\alpha = 8784$ keV, $T_{1/2} = 0.299$ μs)→^{208}Pb. A typical example of such an analysis is presented in Fig. 3, where the β spectrum of ^{212}Bi, the α peak of ^{212}Po and the distribution of the time intervals between the first and the second pulse are depicted.

The energy and time spectra are in a good agreement with those expected for the ^{212}Bi β decay and for the subsequent ^{212}Po α decay. All such double pulses (Fig. 3d) with delay time in the interval $\Delta t = (0.11-0.65)$ μs have been discarded from the raw data to reduce the background. Note that in case of shorter Δt these events are successfully discriminated by the pulse-shape analysis with the optimum digital filter described above. The values of the shape indicator for such the events are lower than those for single γ quanta or β particles.

5. CeF_3 radioactive contaminations

The background spectrum of the CeF_3 crystal measured during 2142 h in the low background set-up is depicted in Fig. 4.

Taking into account the α/β ratio, the wide peak in the energy range (0.6−1.3) MeV may be attributed to the decays of the ^{228}Th and to their α active daughters. The alpha nature of the events, which compose the peak, has been confirmed by the pulse-shape discrimination (see Fig. 2). Moreover, it has also been shown by the time-amplitude analysis of the recorded events (for details see Refs. [7,9]). For example, the fast sequences of the

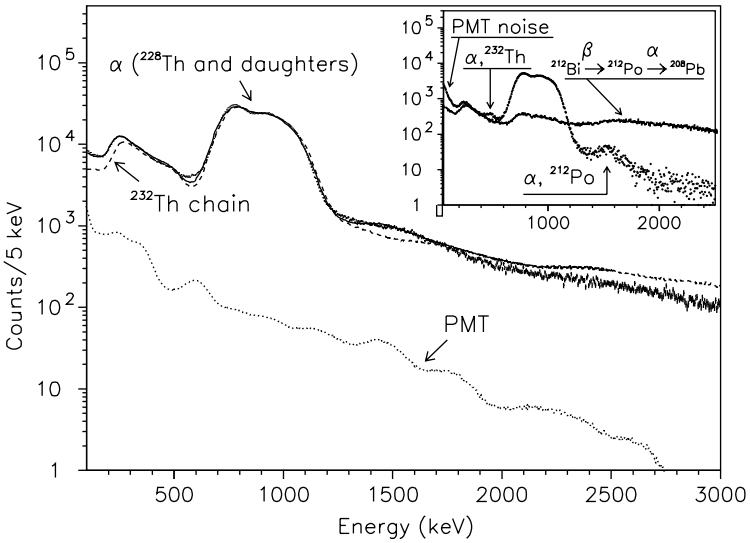

Fig. 4. The energy spectrum of the CeF_3 scintillator of 49.3 g mass measured during 2142 h in the low background set-up. The result of fit (solid line) and the most important background components (internal contamination by ^{232}Th daughter nuclides and external γ radiation from the two PMTs) are presented. In the inset: the energy spectra selected by pulse-shape discrimination (see text) for γ(β) events (solid line) and α events (points) are shown. The differences between the spectra are ascribed to PMT noise contribution in the low energy part and to the events of the $^{212}Bi \rightarrow ^{212}Po \rightarrow ^{208}Pb$ chain for energy above 1.2 MeV. The peak with energy ≈1.55 MeV in α spectrum is caused by α decay of ^{212}Po if energy of ^{212}Bi β particles was below the detector threshold. The peak at the energy (482±12) keV corresponds to activity of ^{232}Th in the crystal at the level of 37(16) mBq/kg.

two α decays from the ^{232}Th family: ^{220}Rn ($E_\alpha =$ 6288 keV, $T_{1/2} = 55.6$ s)→^{216}Po ($E_\alpha = 6788$ keV, $T_{1/2} = 0.145$ s)→^{212}Pb have been selected from the measured data. The energy spectra of the ^{220}Rn and ^{216}Po α particles, obtained in such a way, as well as the distribution of time intervals between the first and the second pulse are presented in Fig. 5. The half-life of ^{216}Po obtained by the fit of this distribution ($T_{1/2} =$ 0.144(2) s) is in agreement with the result from literature [10]. The ^{228}Th activity in the CeF_3 crystal derived from this analysis is equal to 1.01(1) Bq/kg.

Likewise, the broad distribution in the energy range 0.1−0.6 MeV is mainly due to the contamination of the crystal by the β active nuclides from the ^{232}Th family. The β and γ radiation, which follows decays of ^{228}Ac ($Q_\beta = 2127$ keV), ^{212}Pb ($Q_\beta = 574$ keV) and ^{212}Bi ($Q_\beta = 2254$ keV), gives contribution up to 2.3 MeV. The overlapping of the pulses from the fast chain $^{212}Bi \rightarrow ^{212}Po \rightarrow ^{208}Pb$ provides events in the (1.2−4) MeV energy range, while the decays of ^{208}Tl ($Q_\beta = 5001$ keV) contribute up to 5 MeV.

The experimental spectrum was simulated with the help of the GEANT3.21 package [11] and the event generator DECAY4 [12]. Beside the background components described above, the radioactive impurities of the PMTs (which were measured previously [13]) as well as residual PMT noise (exponential function) were also included in the fit. Supposing that equilibrium in the natural radioactive series in the crystal was broken, the least squares fit of the experimental spectrum in the (0.1−2.5) MeV energy region by the sum of the listed components gives the activities (taken as free parameters for the fit) of the intrinsic contaminations of the CeF_3 crystal by ^{232}Th, ^{228}Ra, ^{228}Th, ^{238}U/^{234}U and ^{226}Ra; they are shown in Table 1 and Fig. 4.

As it is visible from the latter, the main part of the background counting rate is caused by daughters of ^{232}Th and radiation from PMT (95 and 2%, respectively). The above procedure has

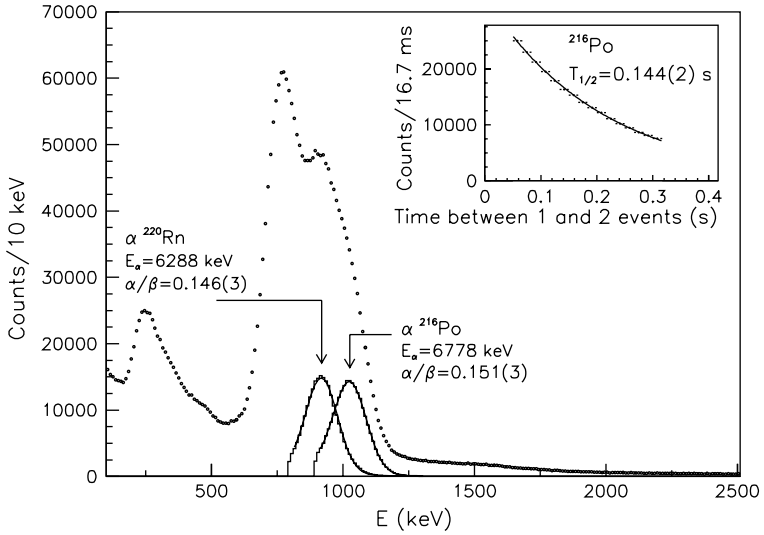

Fig. 5. The background energy spectrum accumulated during 2142 h (points) and spectra of the first and second α particles in the $^{220}Rn \rightarrow ^{216}Po \rightarrow ^{212}Pb$ decay chain as selected by the time-amplitude analysis (histograms). In the inset: the distribution of the time intervals between the first and the second events together with an exponential fit which gives $T_{1/2} = 0.144(2)$ s for ^{216}Po half-life (value from literature is $T_{1/2} = 0.145(2)$ s [10]).

Table 1
Radioactive contaminations in the CeF_3 crystal scintillator obtained by fitting the experimental spectrum by the background model. The derived in this way activity of ^{232}Th 55(30) mBq/kg is consistent with the value of 37(16) mBq/kg obtained by the pulse-shape analysis of the data

Chain	Source	Activity (mBq/kg)
^{232}Th	^{232}Th	55(30)
	^{228}Ra	890(270)
	^{228}Th	1010(10)
^{238}U	^{238}U	$\leqslant 70$
	^{234}U	$\leqslant 60$
	^{230}Th	$\leqslant 60$
	^{226}Ra	$\leqslant 60$
	^{210}Pb	$\leqslant 280$
^{235}U	^{235}U	$\leqslant 40$
	^{231}Pa	$\leqslant 50$
	^{227}Ac	$\leqslant 20$
	^{40}K	$\leqslant 330$
	^{138}La	$\leqslant 60$
	^{176}Lu	$\leqslant 20$
	^{147}Sm	$\leqslant 80$

been repeated including into the background model the following radioactive impurities: ^{230}Th, ^{210}Pb, ^{235}U, ^{231}Pa, ^{227}Ac (and their short-lived daughters), ^{40}K, ^{138}La and ^{176}Lu. The obtained limits on their activities in the crystal are also presented in Table 1.

Unlike the rather high activity of ^{228}Ra and ^{228}Th, the decay rate of ^{232}Th is noticeably low: 55(30) mBq/kg. However, the presence of the ^{232}Th α peak has been confirmed by the pulse-shape analysis of the data; the results are shown in the inset of Fig. 4, where the two energy spectra are depicted. The first one has been selected with condition: $SI < SI_\gamma - 1.6\sigma_\gamma$; it contains $\approx 5.5\%$ of γ(β) events, while α events are practically absent (see inset in Fig. 2). The second spectrum was selected for $SI > SI_\gamma + 1.6\sigma_\gamma$ and it contains $\approx 5.5\%$ of γ(β) events and about (6–9)% of α particles. Apart from the visible difference in the amplitude of the (5.5−6.8) MeV α distributions, these spectra are different in other energy regions. In particular, the increase of the first "gamma/beta" spectrum above 1.2 MeV is due to events from the $^{212}Bi \rightarrow ^{212}Po \rightarrow ^{208}Pb$ sequence. The excess of the second distribution in the low energy part can be explained by PMT noise, while the peak at the ≈ 1.55 MeV energy is caused by the α decay of ^{212}Po if the energy of the foregoing β particle of the ^{212}Bi was below the detector threshold. Besides, a clear small peak is observed

in "alpha" spectrum at the energy (482 ± 12) keV in agreement with an expected position of ^{232}Th alpha peak: (509 ± 25) keV. Corresponding activity of ^{232}Th derived from this pulse-shape analysis is 37(16) mBq/kg. Such a disbalance between ^{232}Th and ^{228}Th (1010 mBq/kg) activities could be explained by broken secular equilibrium of thorium family during crystal growth. Primary mainly ^{228}Ra entered into the crystal and, thereafter, led to ^{228}Th production. Apparently this fact must be taken into account in further development of radiopure CeF_3 crystals.

6. CeF_3 application capability to the search for rare decays of Ce isotopes

In the following the previous results on the performances of the CeF_3 crystal scintillator are exploited to investigate its application capability to the search for rare decays of Ce isotopes.

6.1. *Two neutrino* 2K *capture in* ^{136}*Ce and* ^{138}*Ce*

The two neutrino 2β decays are allowed in the Standard Model (SM) of particle physics and their investigation is important since this could help in the theoretical interpretation of this phenomenon and in the development of experimental methods to study the 0ν2β decay processes, which violate the lepton number conservation and are forbidden in the SM [14]. Furthermore, the 2ν2β decay mode can play the role of an irremovable background in some experiments on 0ν2β decay, solar neutrinos and dark matter.

For two cerium isotopes the capture of two K electrons from the atomic shell with emission of two neutrinos is energetically allowed: (i) $^{136}\mathrm{Ce} \rightarrow {}^{136}\mathrm{Ba}$ (mass difference $\Delta M = 2400(50)$ keV [15]; abundance $\delta = 0.185\%$ [16]; number of ^{136}Ce nuclei in the CeF_3 crystal $N = 2.79 \times 10^{20}$); (ii) $^{138}\mathrm{Ce} \rightarrow {}^{138}\mathrm{Ba}$ (mass difference $\Delta M = 693(10)$ keV; abundance $\delta = 0.251\%$; number of ^{138}Ce nuclei $N = 3.78 \times 10^{20}$). In both such processes the full energy released in the CeF_3 detector is equal to $2E_K$ (where $E_K = 37.4$ keV is the binding energy of electrons on the K shell of Ba atoms), while neutrinos carry out the rest of the available energy ΔM.

The part of the measured distribution up to the energy of 250 keV after the discrimination of the PMT noise and of the double pulses is depicted in Fig. 6a.

To suppress the PMT noise, the events with shape indicator values $SI \geqslant SI_\gamma + 2\sigma_\gamma$ have been discarded from the data. The double pulses have been rejected in two ways: (i) by cutting the couples of events with delay time in the interval $\Delta t = (0.11 - 0.65)$ μs, and (ii) by selecting the events with $SI \leqslant SI_\gamma - 2\sigma_\gamma$ to discriminate pulses with shorter Δt. In the energy interval 30−60 keV the data have been corrected for the decrease of the registration efficiency near threshold, thus the final spectrum includes 95.4% of γ(β) events. The background rate in the energy interval of interest (50−200 keV) has been reduced to 14.7 counts/(h keV kg).

Since in the measured spectrum any peak is absent in the vicinity of the $2E_K$ energy, only limits for the probability of the 2ν2K capture in ^{136}Ce and ^{138}Ce can be set. The half-life limits have been evaluated according to the known formula: $T_{1/2}^{\lim} = \ln 2\, \eta\, N\, t / S^{\lim}$, where N is the number of ^{136}Ce or ^{138}Ce nuclei, η is the detection efficiency, $t = 2142$ h is the measuring time, and $S^{\lim}$ is the number of 2ν2K events which can be excluded at the given confidence level. The response function of the CeF_3 detector for the 2ν2K decay of ^{136}Ce (^{138}Ce) has been simulated with the help of GEANT3.21 and DECAY4 codes and corresponds to a peak (practically a Gaussian) with the center at 72 keV and a width of 45 keV (FWHM). Edge effects slightly shift the peak to lower energy without loss in the detection efficiency. The value of $S^{\lim}$ has been obtained by the least-squares fit of the spectrum in the 60−140 keV energy interval by the sum of the peak searched for and of the background model discussed in Section 5. The fit yields the peak area -23 ± 1079 counts; thus it gives no evidence for the effect. Applying the recommendations of the Particle Data Group [17] we get $S^{\lim} = 1749(1056)$ counts at 90%(68%) C.L. and set the following half-life limits for 2ν2K capture in ^{136}Ce and ^{138}Ce (attributing all the excluded number of

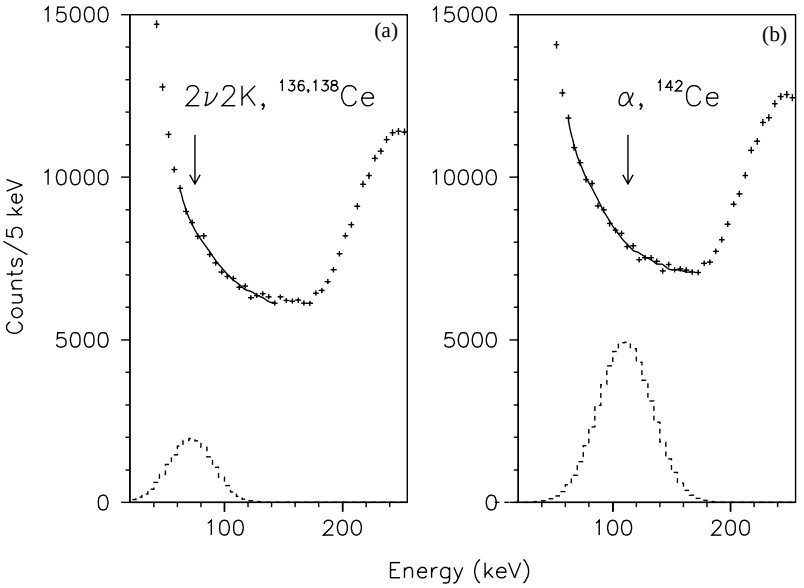

Fig. 6. Low energy part of the background spectra measured during 2142 h in the low background set-up with the CeF_3 scintillator after the pulse-shape discrimination. (a) Spectrum after rejection of PMT noise and double pulses together with fitting curve (see text). Simulated peak of 2v2K capture in ^{136,138}Ce with area $S = 2 \times 10^4$ counts is shown for illustration. (b) The spectrum after rejection of double events which could content at least 99% of ^{142}Ce α peak. The fit of the spectrum is shown by solid line, the simulated α peak of ^{142}Ce corresponding to half-life 5×10^{16} yr (the previous best experimental limit [19])—by dashed line.

events to either first or second isotope):

$$T_{1/2}^{2\nu 2K}(^{136}\mathrm{Ce}) \geqslant 2.7(4.5) \times 10^{16}\ \mathrm{yr} \quad \text{at } 90\%(68\%)\ \text{C.L.},$$

$$T_{1/2}^{2\nu 2K}(^{138}\mathrm{Ce}) \geqslant 3.7(6.1) \times 10^{16}\ \mathrm{yr} \quad \text{at } 90\%(68\%)\ \text{C.L.}$$

In Fig. 6a the fitting curve and the simulated peak of 2v2K capture in ^{136,138}Ce with area $S = 2 \times 10^4$ counts are shown for illustration. The obtained half-life bounds are well below the existing theoretical predictions (see Ref. [18]) for the 2v2K capture of ^{136}Ce ($10^{18}-10^{22}$ yr) and the same can be expected for 2v2K capture of ^{138}Ce, for which calculations are not available; nevertheless they are more than two orders of magnitude higher than those established in previous experiment [9].

6.2. α decay of ^{142}Ce

One of the cerium isotopes, ^{142}Ce, can decay to the ground state of ^{138}Ba with emission of an α particle. The corresponding energy release is equal to 1299.6 ± 3.5 keV [15], thus expected energy of α particle is $E_\alpha = 1263$ keV. The existing experimental limit is: $T_{1/2} \geqslant 5 \times 10^{16}$ yr [19].

The number of ^{142}Ce nuclei (natural abundance $\delta = 11.114\%$ [16]) in our CeF_3 crystal are 1.67×10^{22}. The search for the ^{142}Ce α decay has been performed by using the energy spectrum obtained by discarding the double pulses. Taking into account the α/β ratio, the α peak of ^{142}Ce could be expected at the energy (127 ± 7) keV (with FWHM = 53 keV), where the experimental α spectrum contains at least 99% of α events. A fitting procedure, similar to the one used above to estimate the 2v2K capture, has also been applied to search for the ^{142}Ce α decay. The best fit in the $60-165$ keV energy interval gives a peak's area equal to -790 ± 1010 counts and leads to $S^{\mathrm{lim}} = 972(385)$ counts at 90%(68%) C.L. Thus, the lower bound on the half-life of ^{142}Ce α decay is

$$T_{1/2}^{\alpha}(^{142}\mathrm{Ce}) \geqslant 2.9(7.3) \times 10^{18}\ \mathrm{yr} \quad \text{at } 90\%(68\%)\ \text{C.L.}$$

A part of the experimental distribution together with the fitting curve is presented in Fig. 6b. The simulated α peak of ^{142}Ce with $T_{1/2} = 5 \times 10^{16}$ yr (the previous half-life limit [19]) is also shown for comparison.

It is worth noting that the obtained experimental limit—although significantly higher than that previously available [19]—is still much lower than the existing theoretical estimates, which are in the range of $\sim 10^{27}$ yr [20–22].

7. Conclusions

For the first time the response of a CeF_3 crystal scintillator to α particles has been investigated in the wide (2−8.8) MeV energy region and the capability of a pulse-shape discrimination between α particles and γ quanta has been demonstrated. The study of the residual radioactive contaminants in a similar detector has also been carried out. In addition, the application capability—on the basis of the previous results—of such a detector to the search for some rare processes in Ce isotopes has been investigated obtaining improved experimental limits on the 2ν2K decay mode in ^{136}Ce and ^{138}Ce and on the α activity in ^{142}Ce.

This work has shown that significant improvements in the sensitivity to rare processes in Ce isotopes can be obtained by exploiting the techniques studied here, but also that to achieve more competitive results it is a crucial point to overcome the limitation arising from the residual radioactive impurities in this kind of detector. Purification of scintillators from actinides and their daughters to the level of few μBq/kg (radiopurity level already achieved in cadmium tungstate [7,23] and NaI(Tl) [13]) scintillators could decrease the background at least to few counts/(day keV kg). This—together with the use of enriched ^{136}Ce isotope in the CeF_3 scintillators production—would improve the experimental sensitivity at the level expected from the theoretical predictions.

References

[1] D.F. Anderson, IEEE Trans. Nucl. Sci. NS-36 (1989) 137; W.W. Moses, S.E. Derenzo, IEEE Trans. Nucl. Sci. NS-36 (1989) 173.
[2] D.F. Anderson, Nucl. Instr. and Meth. A 287 (1990) 606; W.W. Moses, S.E. Derenzo, Nucl. Instr. and Meth. A 299 (1990) 51;
M. Kobayashi, et al., Nucl. Instr. and Meth. A 302 (1991) 443;
Crystal Clear Coll., S. Anderson, et al., Nucl. Instr. and Meth. A 332 (1993) 373;
P. Lecoq, et al., IEEE Trans. Nucl. Sci. NS-40 (1993) 409;
M.A. Schneegans, Nucl. Instr. and Meth. A 344 (1994) 47;
R. Chipaux, et al., Nucl. Instr. and Meth. A 345 (1994) 440;
M. Gao, et al., Nucl. Instr. and Meth. A 348 (1994) 163;
E. Auffray, et al., Nucl. Phys. B (Proc. Suppl.) 44 (1995) 57;
E. Auffray, et al., Nucl. Instr. and Meth. A 378 (1996) 171;
E. Auffray, et al., Nucl. Instr. and Meth. A 383 (1996) 367;
I.E. Gursky, et al., Instr. Exp. Tech. 43 (2000) 31;
T. Inagaki, et al., Nucl. Instr. and Meth. A 443 (2000) 126.
[3] R. Bernabei, et al., Il Nuovo Cim. A 110 (1997) 189.
[4] J.B. Birks, Theory and Practice of Scintillation Counting, Pergamon, New York, 1967.
[5] R. Bernabei, et al., Phys. Lett. B 389 (1996) 757.
[6] R. Bernabei, et al., Phys. Lett. B 436 (1998) 379.
[7] F.A. Danevich, et al., Phys. Rev. C 62 (2000) 045 501.
[8] E. Gatti, F. De Martini, Nuclear Electronics, Vol. 2, IAEA, Vienna, 1962, p. 265.
[9] F.A. Danevich, et al., Nucl. Phys. A 694 (2001) 375.
[10] R.B. Firestone, V.S. Shirley, et al. (Eds.), Table of Isotopes, 8th Edition, Wiley, New York, 1996.
[11] GEANT. CERN Program Library Long Write-up W5013, CERN (1994).
[12] O.A. Ponkratenko, et al., Phys. Atomic Nuclei 63 (2000) 1282.
[13] R. Bernabei, et al., Il Nuovo Cim. A 112 (1999) 545.
[14] Yu. Zdesenko, Rev. Mod. Phys. 74 (2002) 663.
[15] G. Audi, A.H. Wapstra, Nucl. Phys. A 595 (1995) 409.
[16] I.L. Barnes, et al., Pure Appl. Chem. 63 (1991) 991.
[17] D.E. Groom, et al., Eur. Phys. J. C 15 (2000) 1.
[18] V.I. Tretyak, Yu.G. Zdesenko, At. Data Nucl. Data Tables 61 (1995) 43;
V.I. Tretyak, Yu.G. Zdesenko, At. Data Nucl. Data Tables 80 (2002) 83.
[19] R.D. Macfarlane, T.P. Kohman, Phys. Rev. 121 (1961) 1758.
[20] B. Al-Bataina, J. Janecke, Phys. Rev. C 37 (1988) 1667.
[21] D.N. Poenaru, M. Ivascu, J. Phys. 44 (1983) 791.
[22] B. Buck, et al., J. Phys. G 17 (1991) 1223.
[23] S.F. Burachas, et al., Nucl. Instr. and Meth. A 369 (1996) 164.